

Section II: Phase Diagram Evaluations

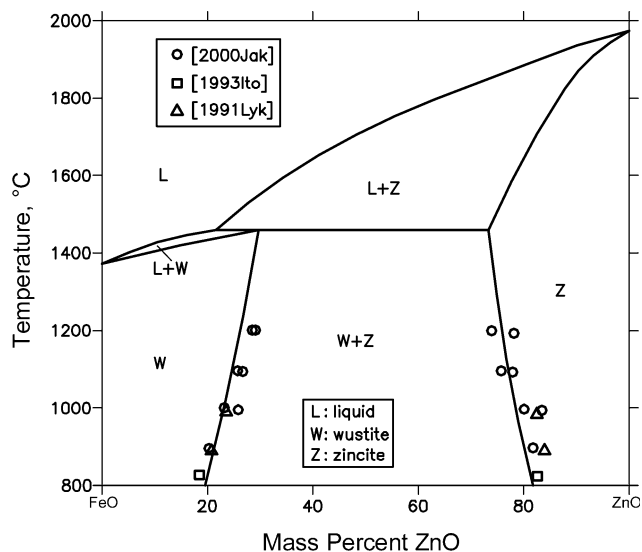


Fig. 2 FeO-ZnO computed vertical section at metallic iron saturation [2001Deg]

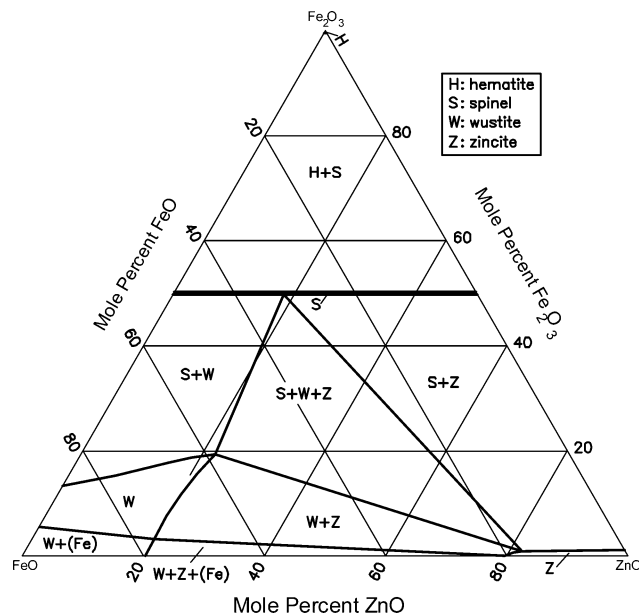


Fig. 4 Fe-O-Zn computed isothermal section at 900 °C on the FeO-Fe₂O₃-ZnO plane [2001Deg]

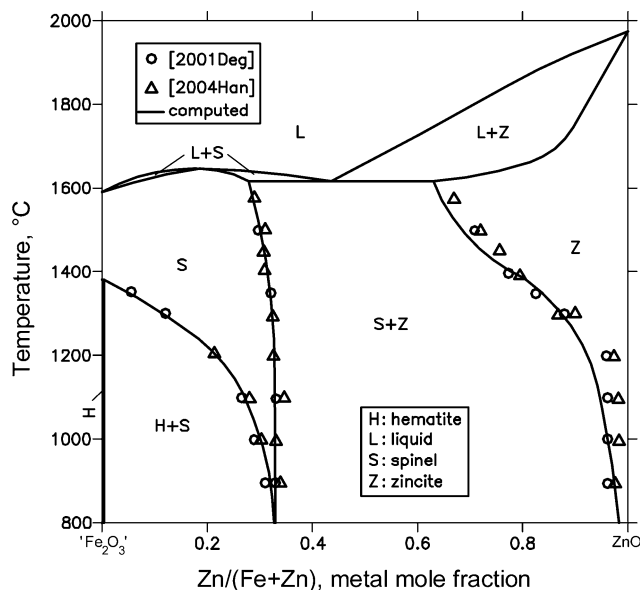


Fig. 3 Fe₂O₃-ZnO computed pseudo-binary section in air [2004Han]

A thermodynamic description for the FeO-Fe₂O₃-ZnO region was developed by [2001Deg] for calculating the phase equilibria. A quasi-chemical model was used for the liquid oxide phase (slag). The spinel structure was described with a three sublattice model. The oxygen anions stay on the fcc sites. The two cations were assumed to be distributed on both the octahedral and the tetrahedral sites. The magnetic contribution to the Gibbs energy was taken into account. For describing the wustite and zincite solution phases, FeO, ZnO, and Fe₂O₃ were taken as the components.

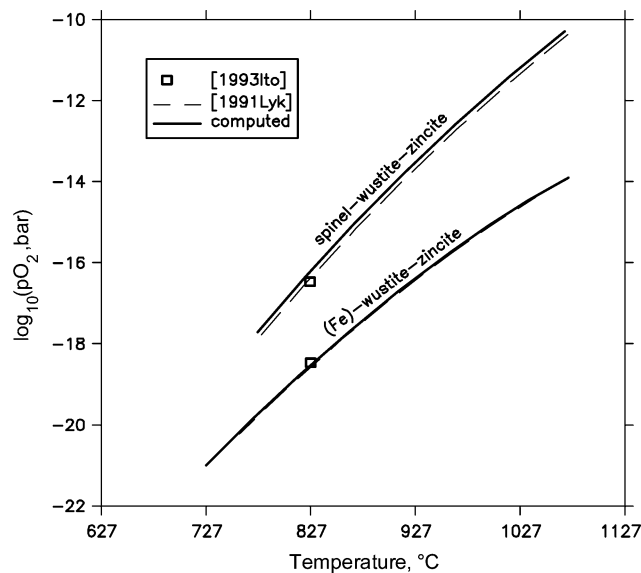


Fig. 5 Fe-O-Zn computed oxygen partial pressures for the indicated three-phase equilibria [2001Deg]

The vertical section calculated by [2001Deg] along the FeO-ZnO join at iron saturation is shown in Fig. 2, along with experimental data of [2000Jak] and earlier workers. Agreement with the experimental results is good. Substantial mutual solid solubility between FeO and ZnO is seen, which increases with increasing temperature. It may be noted that Fe is an additional equilibrium phase in the phase fields in Fig. 2. Figure 3 shows the calculated pseudo-binary section along the ZnO-Fe₂O₃ join [2004Han]. The experimental data of [2001Deg] and [2004Han] show good

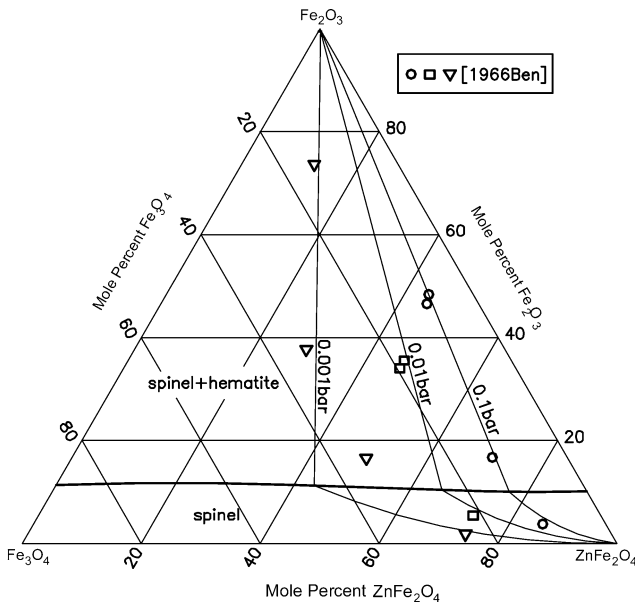


Fig. 6 Fe-O-Zn computed equilibria between spinel and hematite at 1100 °C [2001Deg]

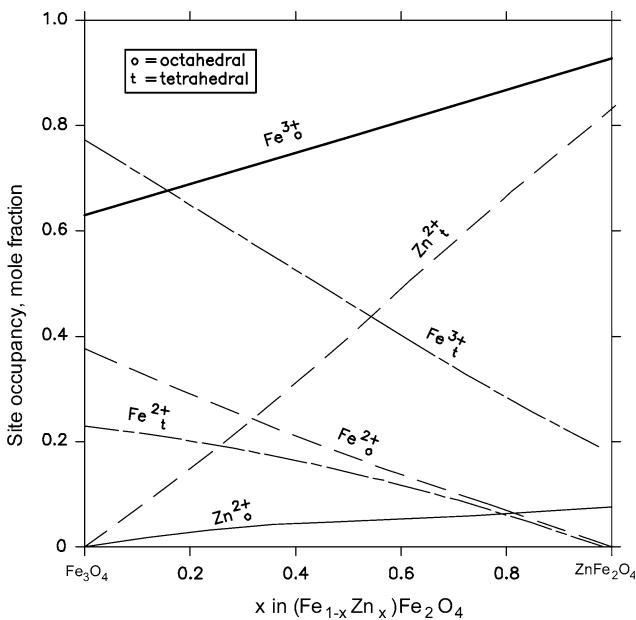


Fig. 7 Fe-O-Zn computed octahedral/tetrahedral distribution of Fe^{2+} , Fe^{3+} , and Zn^{2+} ions in spinel at 900 °C [2001Deg]

agreement with the computed phase diagram. Figure 4 is the calculated isothermal section at 900 °C on the FeO- Fe_2O_3 -ZnO plane [2001Deg]. Fe_2O_3 and $ZnFe_2O_4$ form a continuous solid solution. Zincite dissolves a small amount of Fe_2O_3 . Figure 5 shows the comparison between calculated and experimental oxygen partial pressures as a function of temperature for the three-phase equilibria of (spinel + wustite + zincite) and (iron + wustite + zincite). Figure 6

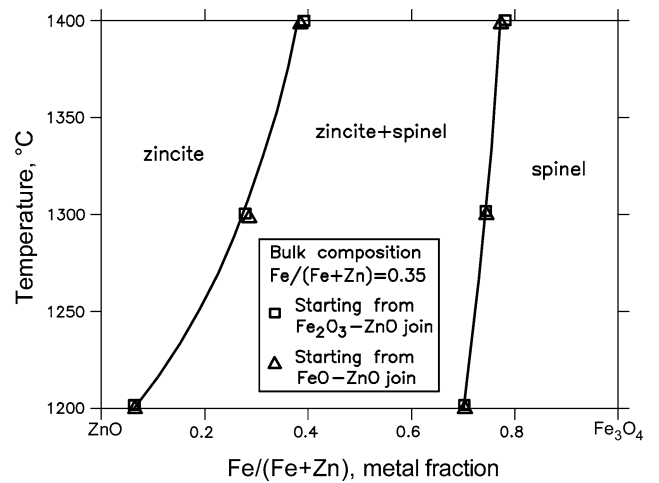


Fig. 8 Fe_3O_4 -ZnO pseudo-binary section at $pO_2 = 10^{-6}$ atm [2005Han]

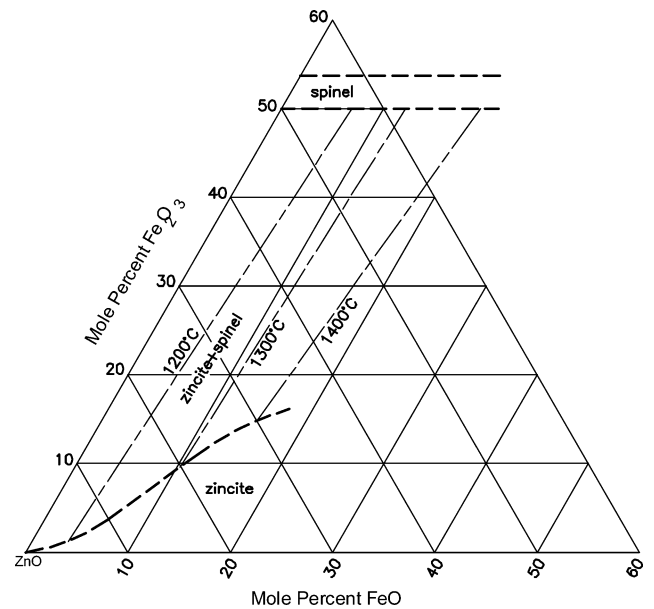


Fig. 9 Fe-O-Zn equilibria between zincite and spinel at $pO_2 = 10^{-6}$ atm and at the indicated temperatures [2005Han]

is an isothermal section at 1100 °C depicting the calculated equilibria between spinel and hematite. The comparison with the experimental data shows good agreement. The predicted octahedral/tetrahedral distribution of Fe^{2+} , Fe^{3+} , and Zn^{2+} ions in spinel at 900 °C is shown in Fig. 7.

For oxygen partial pressures that lie between iron-saturation and air, [2005Han] determined the phase equilibria between 1200 and 1400 °C and between $pO_2 = 10^{-4}$ and 10^{-10} atm. The fixed O_2 pressures were maintained during annealing by flowing known gas mixtures of $H_2/N_2/CO_2$ or CO/CO_2 . The phase equilibria were studied with optical microscopy and electron probe microanalysis. The ferrous/ferric ion concentrations were obtained from wet

Section II: Phase Diagram Evaluations

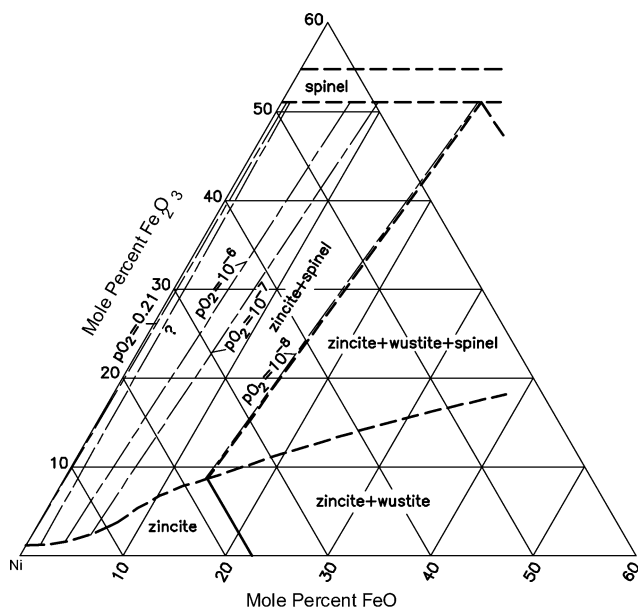


Fig. 10 Fe-O-Zn isothermal section at 1200 °C, showing the pO_2 isobars (atm) [2005Han]

chemical analysis. The pseudo-binary section along the ZnO-Fe₃O₄ join constructed by [2005Han] at $pO_2 = 10^{-6}$ atm is shown in Fig. 8. Figure 9 is an isobaric section at $pO_2 = 10^{-6}$ atm, with the experimental tie-lines between zincite and spinel at 1200, 1300, and 1400 °C. Both ferrous and ferric ion concentrations in zincite increase with increasing temperature. Figure 10 depicts the isothermal section at 1200 °C, showing the experimental pO_2 isobars. The isobar of 10^{-8} atm lies close to the three-phase region of (wustite + zincite + spinel). A full calculated isothermal section at 1200 °C is shown in Fig. 11 as a function of pO_2 (atm) (total pressure = 1 atm) [2005Han].

References

1966Ben: R.L. Benner and H. Kenworthy, Thermodynamic Properties of the ZnO-Fe₂O₃-Fe₃O₄ System at Elevated Temperatures. I. Thermodynamic Properties as Related to the Spinel Solid Solution, *Bureau of Mines (U.S.) Rep. Invest.*, 1966 (6754), p 1-44

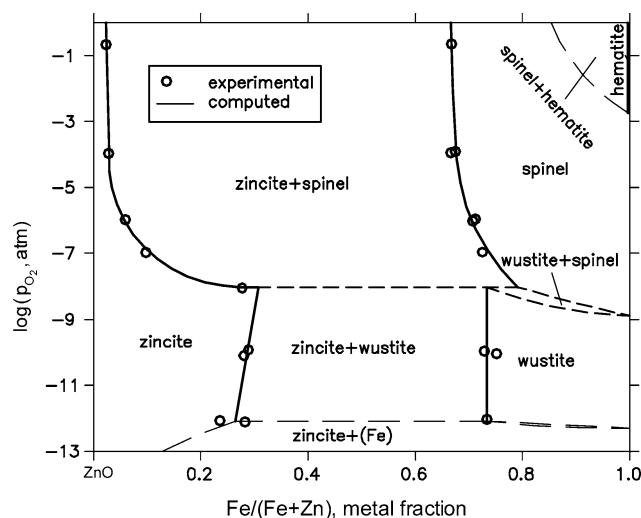


Fig. 11 Fe-O-Zn computed isothermal section at 1200 °C as a function of pO_2 (atm) [2005Han].

1989Rag: V. Raghavan, The Fe-O-Zn (Iron-Oxygen-Zinc) System, *Phase Diagrams of Ternary Iron Alloys, Part 5: Ternary Systems Containing Iron and Oxygen*, Indian Institute of Metals, Calcutta, 1989, p 370-373

1991Lyk: A.A. Lykasov, V.V. D'yachuk, M.S. Pavlovskaya, and T. Popova, Monovariant Equilibria in the Fe-Zn-O System, *Neorg. Mater.*, 1991, **27**(3), p 539-543

1991Wri: H.A. Wriedt, The Fe-O (Iron-Oxygen) System, *J. Phase Equilib.*, 1991, **12**(2), p 170-200

1993Ito: S. Itoh and T. Azakami, Activities of the Components and Phase Relations in Zn-Fe-O and ZnO-FeO-SiO₂ Systems, *Metall. Rev. MMIJ*, 1993, **10**(2), p 113-133

2000Jak: E. Jak, B. Zhao, and P.C. Hayes, Experimental Study of Phase Equilibria in the Systems Fe-Zn-O and Fe-Zn-Si-O at Metallic Iron Saturation, *Metall. Mater. Trans. B*, 2000, **31**, p 1195-1201

2001Deg: S.A. Degterov, E. Jak, P.C. Hayes, and A.D. Pelton, Experimental Study of Phase Equilibria and Thermodynamic Optimization of the Fe-Zn-O System, *Metall. Mater. Trans. B*, 2001, **32**, p 643-657

2004Han: P. Hansson, P.C. Hayes, and E. Jak, Phase Equilibria in the ZnO-Rich Area of the Fe-Zn-O System in Air, *Scand. J. Metall.*, 2004, **33**, p 294-304

2005Han: P. Hansson, P.C. Hayes, and E. Jak, Phase Equilibria in the System Fe-Zn-O at Intermediate Conditions between Metallic-Iron Saturation and Air, *Metall. Mater. Trans. B*, 2005, **36**, p 179-185